NBSIR 76-841

AN ANALYTICAL AND EXPERIMENTAL DETERMINATION OF THE CUTOFF FREQUENCIES OF HIGHER-ORDER TE MODES IN A TEM CELL

John C. Tippet
David C. Chang

University of Colorado

and

Myron L. Crawford

Electromagnetics Division
Institute for Basic Standards
National Bureau of Standards
Boulder, Colorado 80302

June 1976

NBSIR 76-841

AN ANALYTICAL AND EXPERIMENTAL DETERMINATION OF THE CUTOFF FREQUENCIES OF HIGHER-ORDER TE MODES IN A TEM CELL

John C. Tippet
David C. Chang

University of Colorado

and

Myron L. Crawford

Electromagnetics Division
Institute for Basic Standards
National Bureau of Standards
Boulder, Colorado 80302

June 1976

CONTENTS

LIST OF FIGURES AND TABLES

FOREWORD

This report describes the theoretical and experimental determination of the cutoff frequency of the first higher-order mode for several TEM cells of differing geometry developed at the National Bureau of Standards (NBS). In addition, the field distribution of the first higher-order mode is found explicitly.

The effort is part of a program sponsored by the Electronics Systems Division, Hanscom Air Force Base, under contract number Y75-917 with NBS. The purpose of this effort is to evaluate the use of TEM cells for determining the radiated emission characteristics of small electronic devices.

The theoretical analyses were developed by staff from the University of Colorado under contract with NBS. The experimental work was performed at NBS. Myron L. Crawford of the Electromagnetics Division was the technical monitor for NBS and Charles E. Wright of the Electronics Systems Division was the technical monitor for the Air Force. The period of performance covered by this report extends from November 1975 to April 1976.

Results of this effort will be used to develop higher-order mode suppression or rejection techniques to increase the useful frequency range of a TEM cell.

AN ANALYTICAL AND EXPERIMENTAL DETERMINATION OF THE CUTOFF FREQUENCIES
OF HIGHER-ORDER TE MODES IN A TEM CELL

John C. Tippet, David C. Chang and Myron L. Crawford

ABSTRACT

In addition to the TEM mode, higher order TE and TM modes can
propagate in a TEM cell. Since only the TEM mode is desired, the
higher-order modes restrict the useful frequency range of the TEM
cell. In this paper, the cutoff frequency of the first higher-
order mode is obtained both analytically and experimentally for
several TEM cells of differing geometry. The difference between
the experimental and theoretical results is shown to be only a few
percent. In addition the field distribution of the first higher-
order mode is found explicitly.

Key words: Shielded strip line; TEM cell.

1. INTRODUCTION

In our previous report on the TEM cell, an effort was made to investigate
the properties of the dominant TEM mode [1]. In this paper, the first few
nigher-order TE modes in the TEM-cell will be studied. They are of interest
since they determine the upper frequency limit below which only the TEM mode
can propagate. Thus, knowledge of these modes may enable us to increase the
useful frequency range of a TEM-cell, for example, by placing selectively
absorbing material in the cell at locations where the effect is least on the
propagation of the TEM mode.

As is obvious from the sketch shown in figure 1, the TEM cell can be
viewed as a special case of a shielded strip line for which the strip is
embedded in a homogeneous dielectric. Solutions leading to the cutoff fre-
quencies of the higher-order modes in shielded strip line structures usually
involve a numerical search for the roots of an infinite determinant obtained
from a mode matching at the interface between the partial regions separated
by the center septum in the cell. A problem arises, however, since the
infinite determinant must be truncated in order to obtain numerical results.
As Mittra has shown [2], the partitioning of the set of equations (i.e. the
number of modes used in each of the partial regions) must be chosen in the
correct ratio in order that the solution of the truncated set of equations
converges to the correct value. In fact, an incorrect choice of the par-
titioning ratio leads to a violation of the edge condition [3].

In order to bypass the difficulties associated with relative convergence,
an alternative approach was sought in this report. An integral-equation formu-
lation for the electric field in the gap was found, and an approximate, but
analytical solution of the integral equation was obtained using the assumption
of a small gap between the center septum and side walls. (All of the TEM cells
currently in use at NBS indeed have small enough gaps so that the analysis

applied.) This allows us to represent the cutoff frequency of the first higher order mode as a perturbation to the TE_{10} mode in a rectangular waveguide. The method developed in this paper is applicable to TEM cells for which the center septum is displaced vertically from its center position, and may also apply to TEM cells for which the regions above and below the center septum have different dielectric constants (i.e. a shielded strip line). In addition to the cutoff frequencies, the electric field distribution of the higher-order modes can be found explicitly.

In order to check our solution, we compared our results to those obtained by other authors [4,5,6]. In particular, Mittra and Itoh [4] used a singular-integral equation formulation. Their results reduce exactly to ours when a small gap approximation is used in their equations. However, the results obtained by Bräckelmann, et al. [5] and Bezlyudova [6] were not useful for comparison since their result for a zero-thickness septum reduces to the cutoff frequency of the unperturbed TE_{10} mode in a TEM cell, independent of the width of the center septum. If we regard the upper and lower regions of the TEM cell as two rectangular waveguides coupled through a small aperture, then the use of the so-called coupled mode theory predicts that two system modes (symmetric and anti-symmetric) can exist, both of which have approximately the same propagation constant. The symmetric mode is unaffected by the edge condition at the ends of the septum, while the anti-symmetric mode is more strongly affected by the width of the septum [7]. It is clear that the results of Bräckelmann et al. [5] and Bezlyudova [6] were intended for the symmetric mode. However, because the excitation of the TEM cell is basically of a TEM nature which yields an oppositely-directed electric field in the upper and lower regions of the cell, it is more relevant to obtain results corresponding to the anti-symmetric case.

The resonant frequency of the first higher-order perturbed mode was also obtained experimentally in this paper. Using the well-known relationship between the resonant frequency and the cutoff frequency, excellent agreement was obtained between the theoretically and experimentally measured resonant frequencies.

2. FORMULATION OF THE INTEGRAL EQUATION

A cross-section of a TEM cell with an off-center septum is shown in figure 1. The strip, of width 2w, is located a distance g from each vertical sidewall and is assumed to have negligible thickness. In addition it is embedded in a homogeneous dielectric of permittivity, ε_o and permeability, μ_o. The outer wall of the cell, of width 2a and height $2b = b_1 + b_2$, and the strip are assumed to be perfect conductors. The region above the strip is designated region 1 while that below the strip is designated region 2.

We will attempt in this paper to obtain only the cutoff frequencies of the TE-type modes since the TE_{10} mode is usually the lowest order mode next to the dominant TEM-mode in the cell. For the TE modes it is well known that the fields in region 1 can be found in terms of an auxiliary scalar function, $\psi^{(1)}$, which satisfies the following relations.

$$(\nabla_t^2 + K^2)\psi^{(1)} = 0 \qquad \text{in } S_1, \text{ region 1} \tag{1}$$

and

$$\partial_n \psi^{(1)} = 0 \qquad \text{on the metal walls, i.e.,} \atop \text{B-C and A-F-E-D} \tag{2}$$

where

$$K^2 = k_o^2 - \gamma^2; \tag{3}$$

$$k_o^2 = \omega^2 \mu_o \varepsilon_o = \left(\frac{2\pi}{\lambda}\right)^2 ; \tag{4}$$

and we have assumed that the fields propagate as $e^{-i\omega t \pm i\gamma z}$. ∇_t^2 is the transverse Laplacian, which, for our geometry is given by $\partial^2/\partial x^2 + \partial^2/\partial y^2$, and ∂_n represents the outward normal derivative. ω is the angular frequency, λ is the wavelength, k_o is the wave number and γ is the propagation constant which is equal to zero at cutoff. In addition to (2), we will also require that $\partial_n \psi^{(1)}$ be nonzero in the gap regions, that is, A-B and C-D. If $\partial_n \psi^{(1)}$ were zero there also, then we could write the solution to (1) immediately as just an unperturbed rectangular waveguide mode unaffected by the presence of the center septum.

In terms of $\psi^{(1)}$, the field components in region 1 can be written as follows

$$\overline{H}_z = K^2 \psi^{(1)} \overline{a}_z \tag{5}$$

and

$$\overline{E}_t = i\omega\mu_o \nabla_t (\psi^{(1)}) \times \overline{a}_z \tag{6}$$

where $\overline{a}_z$ is a unit vector in the z-direction and ∇_t represents the transverse gradient $(\overline{a}_x \frac{\partial}{\partial x} + \overline{a}_y \frac{\partial}{\partial y})$.

In order to determine $\psi^{(1)}$, we will write it as a superposition of a complete set of basis functions $\psi_{mn}^{(1)}$ as follows

$$\text{In } S_1 \qquad \psi^{(1)} = \sum_{m,n} A_{mn}^{(1)} \psi_{mn}^{(1)}(x,y). \tag{7}$$

$A_{mn}^{(1)}$ are the unknown amplitudes, and the basis functions, $\psi_{mn}^{(1)}$, must satisfy the following

$$\left(\nabla_t^2 + K_{mn}^{(1)^2}\right)\psi_{mn}^{(1)} = 0 \tag{8}$$

3

and

$$\partial_n \psi_{mn}^{(1)} = 0 \tag{9}$$

on ℓ_1, the boundary of S_1, i.e. A-B-C-D-E-F. It may appear that (7) is logically inconsistent since the basis functions, $\psi_{mn}^{(1)}$ satisfy (9) while their sum, $\Psi^{(1)}$ satisfies $\partial_n \Psi^{(1)} \neq 0$ in the gap regions. As shown by Friedman [8], however, $\Psi^{(1)}$ is discontinuous at $y = 0$ and thus the limit $y = 0$ and the sum in (7) cannot be interchanged. In other words, the requirement of $\partial_n \Psi \neq 0$ at the gap should be understood as applied to the plane $y = 0_+$ where $0_+ = \varepsilon$ and $\varepsilon \to 0$. The solution of (8) and (9) is obviously

$$\psi_{mn}^{(1)} (x,y) = \left(\frac{2}{ab_1}\right)^{\frac{1}{2}} \cos\left[\frac{m\pi}{2a} (x+a)\right] \cos\left[\frac{n\pi y}{b_1}\right] \tag{10}$$

with $K_{mn}^{(1)}$ given by

$$K_{mn}^{(1)} = \left[\left(\frac{m\pi}{2a}\right)^2 + \left(\frac{n\pi}{b_1}\right)^2\right]^{\frac{1}{2}} \tag{11}$$

and the normalization constant appearing in (10) is included for convenience.

Using the orthogonality properties of the basis functions, the amplitudes, $A_{mn}^{(1)}$, can be written as follows

$$A_{mn}^{(1)} = \Delta_m \Delta_n \int_{S_1} \Psi^{(1)} (x',y') \psi_{mn}^{(1)} (x',y') \, ds' \tag{12}$$

where

$$\Delta_i = \begin{cases} \frac{1}{2} & i = 0 \\ 1 & \text{otherwise.} \end{cases} \tag{13}$$

In order to find an alternative expression for the surface integral appearing in (12), we multiply (1) by $\psi_{mn}^{(1)}$ and (8) by $\Psi^{(1)}$. Subtracting the resulting equations and integrating over S_1, we obtain the following

$$(K_{mn}^{(1)^2} - K^2) \int_{S_1} \Psi^{(1)} \psi_{mn}^{(1)} \, ds = \int_{S_1} [\psi_{mn}^{(1)} \nabla_t^2 \Psi^{(1)} - \Psi^{(1)} \nabla_t^2 \psi_{mn}^{(1)}] \, ds . \tag{14}$$

Using the two-dimensional form of the divergence theorem and Green's second identity [9], the right-hand-side of (14) can be written as

$$\text{R.H.S.} = \oint_{\ell_1} [\psi_{mn}^{(1)} \partial_n \Psi^{(1)} - \Psi^{(1)} \partial_n \psi_{mn}^{(1)}] \, d\ell . \tag{15}$$

The second term in (15) is zero by virtue of (9). Thus the unknown amplitudes given in (12) reduce to

$$A_{mn}^{(1)} = \frac{\Delta_m \Delta_n}{(K_{mn}^{(1)^2} - K^2)} \oint_{\ell_1} \psi_{mn}^{(1)} \partial_n \Psi^{(1)} \, d\ell . \tag{16}$$

4

Because of (2), however, the line integral in (16) only contributes in the gap. Thus,

$$\oint_{\ell_1} \psi_{mn}^{(1)} \partial_n \psi^{(1)} \, d\ell = -\left(\int_{-a}^{-w} + \int_{w}^{a} \right) \psi_{mn}^{(1)}(x,0) \partial_y \psi^{(1)}(x,0) \, dx \qquad (17)$$

since

$$\partial_n \psi^{(1)} = -\frac{\partial}{\partial y} \psi^{(1)} \qquad \text{at } y = 0. \qquad (18)$$

In order to combine the two integrations appearing in (17), we will consider two cases: (1) the odd modes for which $\psi^{(1)}(x,y) = -\psi^{(1)}(-x,y)$; and (2) the even modes for which $\psi^{(1)}(x,y) = \psi^{(1)}(-x,y)$. The following analysis will apply for the odd modes for which (17) can be written as

$$\oint_{\ell_1} \psi_{mn}^{(1)} \partial_n \psi^{(1)} \, d\ell = -\int_{w}^{a} \partial_y \psi^{(1)}(x,0) \, [\psi_{mn}^{(1)}(x,0) - \psi_{mn}^{(1)}(-x,0)] \, dx. \qquad (19)$$

The term in the square brackets in (19) is zero if m is even. Thus (16) gives

$$A_{mn}^{(1)} = \begin{cases} \dfrac{2\Delta_n}{(K^2 - K_{mn}^{(1)^2})} \displaystyle\int_{w}^{a} \partial_y \psi^{(1)}(x,0) \psi_{mn}^{(1)}(x,0) \, dx & (m=1,3,5,\ldots) \\[4mm] 0 & (m=0,2,4,\ldots). \end{cases} \qquad (20)$$

Equation (20) can now be inserted into (7) which then determines the scalar function, $\psi^{(1)}$ in region 1 in terms of the unknown cutoff wave number, K, and an integration of the unknown electric field in the gap $(\partial_y \psi^{(1)}(x,0) \propto E_x(x,0))$. Thus

$$\psi^{(1)}(x,y) = 2 \sum_{p,n} \frac{\Delta_n}{(K^2 - K_{2p+1,n}^{(1)^2})} \psi_{2p+1,n}^{(1)}(x,y) \int_{w}^{a} \partial_y \psi^{(1)}(x',0) \psi_{2p+1,n}^{(1)}(x',0) \, dx'$$

where p = 0, 1, 2, ... $\qquad (21)$

A similar relation can be written in region 2 by replacing all subscripts and superscripts 2 by 1 and by replacing y by -y. In the gap, we require continuity of H_z and E_x which is equivalent to requiring the following

$$\psi^{(1)}(x,0) = \psi^{(2)}(x,0) \qquad (w < x < a) \qquad (22)$$

and

$$\partial_y \psi^{(1)}(x,0) = \partial_y \psi^{(2)}(x,0) \qquad (w < x < a). \qquad (23)$$

When (22) and (23) are imposed on (21) and its equivalent expression in region 2, we obtain the following integral equation.

$$\int_{w}^{a} \partial_y \psi(x',0) G_o(x,x') \, dx' = 0 \qquad (w < x < a) \qquad (24)$$

5

where

$$G_o(x,x') = \sum_{j=1}^{2} \sum_{p,n} \frac{\Delta_n}{(K^2 - K_{2p+1,n}^{(j)\,2})} \psi_{2p+1}(x,0)\,\psi_{2p+1}(x',0) \tag{25}$$

and we have dropped the superscript on $\partial_y \Psi(x',0)$ since it is continuous across the gap as well as the subscript "n" on the basis functions since they are evaluated at $y = 0$. The Green's function given in (25) is singular at $x = x'$. Thus, as shown in [10, pp. 197-198] the integral equation (24) is to be interpreted in the principal value sense.

A similar expression can be obtained for the even modes. The resulting integral equation is identical to (24) if we replace G_o by G_e which is given as

$$G_e(x,x') = \sum_{j=1}^{2} \sum_{p,n} \frac{\Delta_p \Delta_n}{(K^2 - K_{2p,n}^{(j)2})} \psi_{2p}(x,0)\,\psi_{2p}(x',0). \tag{26}$$

If the septum is located in the center of the TEM cell (i.e. $b_1 = b_2 = b$) then the summation on "j" in (25) and (26) can be dropped and replaced by the factor 2.

3.   SMALL GAP APPROXIMATION FOR THE GREEN'S FUNCTIONS

The integral equation given in (24) could be solved numerically at this point using, for example, the moment method. In this method, the unknown function, $\partial_y \Psi(x',0)$, can be approximated by an M-term Fourier series. Using the orthogonality properties of the basis functions, an M x M matrix equation ensues, and the requirement that the determinant vanish then determines the cutoff frequencies of the higher-order modes. However, since a strictly numerical technique does not furnish much insight as to how the cutoff frequencies change as the gap varies and may also lead to relative convergence difficulties [11], we will solve (24) by approximating the Green's function using a small gap assumption, i.e. $Kg \ll 1$. The solution to the approximate integral equation can then be obtained analytically.

In order to find an approximation for G_o, we note that the summation on "n" in (25) can be written as follows

$$\sum_{n=0}^{\infty} \frac{\Delta_n}{[K^2 - K_{2p+1,n}^{(j)\,2}]} = \left(\frac{b_j}{\pi}\right)^2 \left[\frac{1}{2\alpha_{2p+1}^{(j)2}} - \sum_{n=1}^{\infty} \frac{1}{(n^2 - \alpha_{2p+1}^{(j)2})}\right] \tag{27}$$

where

$$\alpha_{2p+1}^{(j)} \equiv \left(\frac{b_j}{\pi}\right) \left[K^2 - (2p+1)^2 \left(\frac{\pi}{2a}\right)^2\right]^{\frac{1}{2}}. \tag{28}$$

6

The summation on the right-hand-side of (27) is given as [12]

$$\sum_{n=1}^{\infty} \frac{1}{(n^2 - \alpha_{2p+1}^{(j)2})} = \frac{1}{2\alpha_{2p+1}^{(j)2}} - \frac{\pi}{2\,\alpha_{2p+1}^{(j)}} \cot(\pi\,\alpha_{2p+1}^{(j)}) \tag{29}$$

so that (27) reduces to

$$\sum_{n=0}^{\infty} \frac{\Delta_n}{[K^2 - K_{2p+1,n}^{(j)\,2}]} = \frac{b_j^2}{2\pi\,\alpha_{2p+1}^{(j)}} \cot(\pi\,\alpha_{2p+1}^{(j)}). \tag{30}$$

Thus, G_o given in (25) can be written as

$$G_o(x,x') = \sum_{j=1}^{2} \frac{b_j^2}{2\pi} \sum_{p} \frac{\cot(\pi\alpha_{2p+1}^{(j)})}{\alpha_{2p+1}^{(j)}} \psi_{2p+1}(x,0)\psi_{2p+1}(x',0). \tag{31}$$

The summation on "p" in (31) cannot be done in closed-form; however, we notice that for large "p"

$$\frac{\cot(\pi\alpha_{2p+1}^{(j)})}{\alpha_{2p+1}^{(j)}} \sim - \left(\frac{2a}{b_j}\right) \frac{1}{(2p+1)} \tag{32}$$

so that if we add and subtract the right-hand-side of (32) to G_o we obtain the following

$$G_o(x,x') = G_o^{(1)}(x,x') + G_o^{(2)}(x,x') \tag{33}$$

where

$$G_o^{(1)}(x,x') = \sum_{j=1}^{2} \frac{b_j^2}{2\pi} \left(-\frac{2a}{b_j}\right) \sum_{p} \frac{\psi_{2p+1}(x,0)\psi_{2p+1}(x',0)}{(2p+1)} \tag{34}$$

and

$$G_o^{(2)}(x,x') = \sum_{j=1}^{2} \frac{b_j^2}{2\pi} \sum_{p} \left[\frac{\cot(\pi\alpha_{2p+1}^{(j)})}{\alpha_{2p+1}^{(j)}} + \left(\frac{2a}{b_j}\right) \frac{1}{(2p+1)}\right] \psi_{2p+1}(x,0)\psi_{2p+1}(x',0). \tag{35}$$

The term in the square brackets in (35) now decays rapidly as p^{-2}. Hence, $G_o^{(2)}$ approaches a constant whenever $|x-x'| \to 0$. On the other hand, the terms involved in $G_o^{(1)}$ decay only as p^{-1} and thus will have a logarithmic singularity as $|x-x'| \to 0$. Therefore under the assumption of a small gap the dominant contribution to G_o will come from $G_o^{(1)}$.

Substituting for the basis functions from (10), and making the following change of variables

$$t = a - x \tag{36}$$

and

$$t' = a - x' \tag{37}$$

7

$G_O^{(1)}$ can be written as

$$G_O^{(1)}(t,t') = -\frac{2}{\pi} \sum_{p=0}^{\infty} \frac{2}{(2p+1)} \left\{ \cos\left[\frac{(2p+1)\pi(t+t')}{2a}\right] + \cos\left[\frac{(2p+1)\pi(t-t')}{2a}\right] \right\} \qquad (38)$$

which can be summed as [13]

$$G_O^{(1)}(t,t') = \frac{2}{\pi}\left\{ \ln\,\tan\left[\frac{\pi}{4a}\,|t+t'|\right] + \ln\,\tan\left[\frac{\pi}{4a}\,|t-t'|\right] \right\}. \qquad (39)$$

The largest value of $|t+t'|$ is $2g$ so that if we assume that $g/a \ll 1$ we can replace the tangents in (39) by their arguments and obtain

$$G_O^{(1)}(t,t') \simeq \frac{2}{\pi}\,\ln\left[\left(\frac{\pi}{4a}\right)^2\,|t^2-t'^2|\right] \qquad \left(\frac{g}{a} \ll 1\right). \qquad (40)$$

In order to obtain an approximate form for $G_O^{(2)}$ we notice that if we restrict attention to only the first few higher-order modes for which K is not too large, then the sum in (35) converges very rapidly, so rapidly in fact that the arguments of the cosines appearing in the basis functions in (35) remain close to zero. Thus, $G_O^{(2)}$ is essentially independent of x and x' for $gK \to 0$ and we can write

$$G_O^{(2)} \simeq \sum_{j=1}^{2} \frac{1}{\pi} \frac{b_j}{a} \sum_{p=0}^{\infty} \left[\frac{\cot(\pi\alpha_{2p+1}^{(j)})}{\alpha_{2p+1}^{(j)}} + \left(\frac{2a}{b_j}\right) \frac{1}{(2p+1)} \right]. \qquad (41)$$

$$(2gK \ll 1) \qquad (42)$$

Since we have assumed a small gap, it seems reasonable to represent the modes in the TEM cell as perturbations of rectangular waveguide modes; that is, we let

$$K^2 = K_{qr}^{(s)\,2} + \delta_{qr}^{(s)\,2} \qquad (q=1,3,5\ldots) \qquad (r=0,1,2\ldots.) \qquad (s=1,2) \qquad (43)$$

with

$$\delta_{qr}^{(s)} \ll K_{qr}^{(s)} \qquad (44)$$

and $K_{qr}^{(s)}$ cannot be so large that (42) is violated. Then the main contribution to the summation in (41) occurs when $\alpha_{2p+1}^{(j)} \simeq n$ or when $K \simeq K_{2p+1,n}^{(j)}$. There may be more than one term for which this occurs since it is possible to have two or more rectangular waveguide modes with the same cutoff frequency. We will take, for example, $q = 1$ and $r = 0$ which corresponds to a perturbation of the TE_{10} mode in a rectangular waveguide which is the first higher-order mode that we would expect to appear. $K_{qr}^{(s)}$ does not depend on "s" in this case since $r = 0$, and only one term in (41) is dominant. For this case, $G_O^{(2)}$ can be written as

$$(G_O^{(2)})_{TE_{10}} \simeq \sum_{j=1}^{2} \left\{ \left[\frac{\cot(b_j\delta_{10})}{a\delta_{10}} + \frac{2}{\pi}\right] + \frac{2}{\pi} \sum_{p=1}^{\infty} \frac{1}{(2p+1)} \left[1 - \coth\frac{\pi b_j}{2a}(2p+1)\right] \right\}. \qquad (45)$$

8

The summation on "p" in (45) is very small compared to the dominant $p = 0$ term, so we will neglect it, subject to a consistency check when δ_{10} is determined. In any case the summation is rapidly convergent and can be evaluated numerically if needed. Thus,

$$(G_o^{(2)})_{TE_{10}} \simeq \frac{4}{\pi} + \frac{\cot b_1 \delta_{10} + \cot b_2 \delta_{10}}{a \delta_{10}}. \tag{46}$$

In the general case for non-degenerate odd modes, we obtain in a similar way

$$(G_o^{(2)})_{TE_{qr}^{(s)}} \simeq \sum_{j=1}^{2} \left\{ \left[\frac{\cot(b_j \xi_{qr}^{(s)})}{\xi_{qr}^{(s)}} + \frac{2}{\pi q} \right] + \frac{2}{\pi} \sum_{p=0}^{\infty} \frac{1}{(2p+1)} \left[1 - \coth \frac{\pi b_j}{2a} (2p+1) \right] \right\}$$

$$p \neq \frac{(q-1)}{2} \tag{47}$$

where

$$\xi_{qr}^{(s)} = \left[\left(\frac{n\pi}{b_j} \right)^2 + \delta_{qr}^{(s)2} \right]^{\frac{1}{2}}. \tag{48}$$

The preceding analysis has dealt with the approximation of G_o. A similar analysis also applies for G_e, and we therefore only quote the results.

$$G_e^{(1)}(t,t') \simeq \frac{1}{\pi} \ln \left[\left(\frac{\pi}{a} \right)^2 |t^2 - t'^2| \right] \tag{49}$$

and in the general case for non-degenerate even modes we obtain

$$(G_e^{(2)})_{TE_{qr}^{(s)}} \simeq \sum_{j=1}^{2} \left\{ \left[\frac{\cot(b_j \xi_{qr}^{(s)})}{\xi_{qr}^{(s)}} + \frac{2}{\pi q} \right] + \frac{2}{\pi} \sum_{\substack{p=1 \\ p \neq q/2}}^{\infty} \frac{1}{p} \left[1 - \coth \frac{\pi b_j p}{a} \right] + \frac{2}{\pi} \frac{\cot \left(\frac{q\pi b_j}{2a} \right)}{q} \right\}. \tag{50}$$

It is interesting to note that all of the dependence on position (through the variables t and t') is contained in $G_{o,e}^{(1)}$ while all of the dependence on the as yet undetermined K (through $\delta_{qr}^{(s)}$) is contained in $G_{o,e}^{(2)}$.

4. SOLUTION OF THE APPROXIMATE INTEGRAL EQUATION

4.1 Cutoff Frequencies of the Higher-Order Modes

Inserting the approximate form for G_o into (24) we obtain

$$\int_0^g f(t') \left\{ \frac{1}{\pi} \ln \left[\left(\frac{\pi}{4a} \right)^2 |t^2 - t'^2| \right] + G_o^{(2)} \right\} dt' = 0 \tag{51}$$

where

$$f(t') \equiv \partial_y \Psi(a-t',0). \tag{52}$$

9

If we make the following substitutions

$$u = \frac{\pi t}{4a};$$ (53)

$$u' = \frac{\pi t'}{4a};$$ (54)

$$u_o = \frac{\pi g}{4a};$$ (55)

$$A_o = \int_o^g g(t')\, dt;$$ (56)

$$h(u') \equiv \dot{f}(\frac{4au'}{\pi});$$ (57)

then (51) reduces to

$$\int_o^{u_o} h(u')\, \ln|u^2 - u'^2|\, du' = -\frac{\pi^2}{4a}\, G_o^{(2)} A_o.$$ (58)

But the solution of (58) is known to be [14]

$$h(u') = \frac{C}{[u_o^2 - u'^2]^{\frac{1}{2}}}$$ (59)

where C is an arbitrary constant which is related to A_o defined in (56). Inserting (59) into (58) we obtain

$$\int_o^{u_o} \frac{C}{[u_o^2 - u'^2]^{\frac{1}{2}}}\, \ln|u^2 - u'^2|\, du' = \frac{-\pi^2}{4a}\, G_o^{(2)} A_o$$ (60)

which can be written alternatively as follows

$$\int_{-u_o}^{u_o} \frac{C}{[u_o^2 - u'^2]^{\frac{1}{2}}}\, \ln|u - u'|\, du' = \frac{-\pi^2}{4a}\, G_o^{(2)} A_o.$$ (61)

If we make the following substitutions

$$u = u_o \cos\theta$$ (62)

and

$$u' = u_o \cos\phi$$ (63)

then (61) reduces to

$$C \int_o^{\pi} \ln[u_o |\cos\theta - \cos\phi|]\, d\phi = \frac{-\pi^2}{4a}\, G_o^{(2)} A_o.$$ (64)

However, since [10, p. 171]

$$\ln|\cos\theta - \cos\phi| = -\ln 2 - 2 \sum_{m=1}^{\infty} \frac{1}{m} \cos m\theta \cos m\phi$$ (65)

10

(64) reduces to

$$\pi C \ln\left(\frac{u_o}{2}\right) = \frac{-\pi^2}{4a} \, G_o^{(2)} A_o.$$

(66)

A_o in (66) can be found in terms of C by changing variables and substituting (59) into (56) with the result that

$$A_o = 2aC.$$

(67)

Thus, (66) and (67) give

$$\frac{G_o^{(2)}}{2} + \frac{1}{\pi} \ln\left(\frac{u_o}{2}\right) = 0.$$

(68)

Substituting for $G_o^{(2)}$ and u_o from (46) and (55) respectively we obtain the following characteristic equation for the perturbed TE_{10} mode.

$$\frac{1}{2}[\cot b_1 \delta_{10} + \cot b_2 \delta_{10}] = \frac{a\delta_{10}}{\pi}[\ln(\frac{8a}{\pi g}) - 2].$$

(69)

Provided that the remaining sum in (45) is indeed small under the small gap assumption, this is then the equation for determining δ_{10}. In particular, when the gap ratio (g/a) is much smaller than one, the perturbation solution can be obtained simply from the small argument expansion of the cotangent to yield

$$\delta_{10}^2 \simeq \frac{\pi b/a}{b_1 b_2 \ln(\frac{8a}{\pi g})}$$

(70)

and from (43) the cutoff wavenumber is then given by

$$K \simeq \left[\frac{\pi}{2a} + \frac{\pi b/a}{b_1 b_2 \ln(\frac{8a}{\pi g})}\right]^{\frac{1}{2}}.$$

(71)

It is of interest to point out that the form of K as given by (71) is essentially the same as the one obtained in [15] which treats a similar problem in which coupling occurs through only one aperture.

As a trial solution for any numerical or graphical search of the root of (69), we note that since the value of the cotangent can vary from ∞ to 0 when $b_1 \delta_{10}$ increases from 0 to $\pi/2$ (assuming $b_1 > b_2$), the expected solution therefore lies in the range where δ_{10} varies from 0 to $\pi/2b$, which is the midpoint between the unperturbed TE_{10} mode and the unperturbed TE_{20} mode. For g/a ratios from .01 to .3 and a/b ratios from .5 to 1, a nomographic solution of (69) was obtained which allows one to easily determine the cut-off wavelength graphically. This is included in figure 2.

The integral equation with G_e instead of G_o is identical if we replace "a" by a/4. Thus, for example, for the perturbed TE_{20} mode we obtain

$$\frac{1}{2}[\cot b_1 \delta_{20} + b_2 \delta_{20}] = \frac{a\delta_{20}}{4\pi}[\ln(\frac{2a}{\pi g}) - 2]$$

(72)

from which the perturbed cutoff wavenumber can be obtained as above.

11

4.2   Field Distribution of the Higher Order Modes

The field distribution of the higher-order modes can be obtained by substituting the aperture field found in (59) into (21), but first we can evaluate advantageously the unknown constant, C, in terms of the "voltage" drop across the gap.   Substituting for $f(t')$ from (52) into (56) and realizing from (6) that

$$\partial_y \Psi(x',0) = \frac{E_x(x',0)}{i\omega\mu_o} \tag{73}$$

we obtain for A_o.

$$A_o = \frac{1}{i\omega\mu_o} \int_{a-g}^{a} E_x(x',0)\,dx' = \frac{iV}{\omega\mu_o} \tag{74}$$

where V is the potential difference across the gap.   Thus, C in (67) is given as

$$C = \frac{iV}{2a\omega\mu_o} \tag{75}$$

and the aperture field from (59) can then be written as

$$h(u') = \frac{iV}{2a\omega\mu_o}\,[u_o^2 - u'^2]^{-\frac{1}{2}}. \tag{76}$$

Transforming the integration in (21) from x' to u' via (37) and (54) and inserting $h(u')$ from (76) we obtain

$$\int_w^a \partial_y\Psi^{(1)}(x',0)\,\psi_{2p+1}^{(1)}(x',0)\,dx' = -\frac{2}{\pi}\left(\frac{2}{ab_1}\right)^{\frac{1}{2}}\left(\frac{iV}{\omega\mu_o}\right)\int_0^{u_o}\frac{\cos[(2p+1)2u']\,du'}{\sqrt{u_o^2 - u'^2}}, \tag{77}$$

but   the integration in (77) is given as [16]

$$\int_0^{u_o}\frac{\cos[(2p+1)2u']\,du'}{\sqrt{u_o^2 - u'^2}} = \frac{\pi}{2}\,J_o[2(2p+1)u_o]$$

$$= \frac{\pi}{2}\,J_o[(2p+1)\,\frac{\pi g}{2a}] \tag{78}$$

where J_o is a Bessel function of order zero.   Thus by analogy with (21) the fields in regions 1 and 2 can be written as

$$\Psi^{(j)}(x,y) = \left(\frac{4}{ab_j}\right)\left(\frac{iV}{\omega\mu_o}\right)\sum_{p,n}\frac{\Delta_n(-1)^p\,J_o[(2p+1)\frac{\pi g}{2a}]\sin[(2p+1)\frac{\pi x}{2a}]\cos(\frac{n\pi y}{b_j})}{(K^2 - K_{2p+1,n}^{(j)2})} \quad (j=1,2). \tag{79}$$

The summation on "n" in (79) can be written as follows

$$\sum_{n=0}^{\infty}\frac{\Delta_n\cos\left(\frac{n\pi y}{b_j}\right)}{(K^2 - K_{2p+1,n}^{(j)2})} = \left(\frac{b_j}{\pi}\right)^2\left[\frac{1}{2a_{2p+1}^{(j)2}} - \sum_{n=1}^{\infty}\frac{\cos\left(\frac{n\pi y}{b_j}\right)}{(n^2 - a_{2p+1}^{(j)2})}\right] \tag{80}$$

where $\alpha_{2p+1}^{(j)}$ was defined in (28). The summation on the right-hand-side of (80) is given as [12]

$$\sum_{n=1}^{\infty} \frac{\cos\left(\frac{n\pi y}{b_j}\right)}{(n^2 - \alpha_{2p+1}^{(j)2})} = \frac{1}{2\alpha_{2p+1}^{(j)2}} - \frac{\pi}{2\alpha_{2p+1}^{(j)}} \frac{\cos\left[\left(\frac{y}{b_j}\mp1\right)\pi\alpha_{2p+1}^{(j)}\right]}{\sin(\pi\alpha_{2p+1}^{(j)})} \tag{81}$$

so that (79) reduces to

$$\psi^{(j)}(x,y) = \left(\frac{2b_j}{\pi a}\right)\left(\frac{iV}{\omega\mu_o}\right) \sum_{p=0}^{\infty} \frac{(-1)^P J_o\left[(2p+1)\frac{\pi g}{2a}\right]\sin\left[(2p+1)\frac{\pi x}{2a}\right]}{\alpha_{2p+1}^{(j)}} \frac{\cos\left[\left(\frac{y}{b_j}\mp1\right)\pi\alpha_{2p+1}^{(j)}\right]}{\sin(\pi\alpha_{2p+1}^{(j)})}. \tag{82}$$

From (28) and (43) we have that $\alpha_1^{(j)} \simeq \frac{b_j\delta_{10}}{\pi}$ for $r = 0$ so that restricting attention to the perturbed TE_{10} mode we have

$$\psi^{(j)}(x,y) \simeq \left(\frac{2}{a\delta_{10}}\right)\left(\frac{iV}{\omega\mu_o}\right)\frac{\cos[\delta_{10}(y\mp b_j)]}{\sin \delta_{10}b_j}\sin\left(\frac{\pi x}{2a}\right)$$

$$+ \left(\frac{2b_j}{\pi a}\right)\left(\frac{iV}{\omega\mu_o}\right)\sum_{p=1}^{\infty}\frac{(-1)^P J_o\left[(2p+1)\frac{\pi g}{2a}\right]\sin\left[(2p+1)\frac{\pi x}{2a}\right]}{\alpha_{2p+1}^{(j)}}\frac{\cos\left[\left(\frac{y}{b_j}\mp1\right)\pi\alpha_{2p+1}^{(j)}\right]}{\sin(\pi\alpha_{2p+1}^{(j)})}. \tag{83}$$

Since the potential difference, V, is still arbitrary, we can normalize V in such a way that the amplitude of $\sin(\frac{\pi x}{2a})$ is unity with the result that

$$\psi^{(j)}(x,y) = \sin\left(\frac{\pi x}{2a}\right) + \frac{b_j\delta_{10}}{\pi}\frac{\sin \delta_{10}b_j}{\cos[\delta_{10}(y\mp b_j)]}Q \tag{84}$$

where

$$Q = \sum_{p=1}^{\infty}\frac{(-1)^P J_o\left[(2p+1)\frac{\pi g}{2a}\right]\sin\left[(2p+1)\frac{\pi x}{2a}\right]\cos\left[\left(\frac{y}{b_j}\mp1\right)\pi\alpha_{2p+1}^{(j)}\right]}{\alpha_{2p+1}^{(j)}\sin(\pi\alpha_{2p+1}^{(j)})} \qquad (j = 1,2). \tag{85}$$

In this form the first term in (84) can be recognized as the dominant TE_{10} mode of a rectangular waveguide and the second term as a small perturbation. As $g/a \to 0$, $\delta_{10} \to 0$, and the perturbation term in (84) vanishes.

5. EXPERIMENTAL DETERMINATION OF THE RESONANT FREQUENCIES OF TEM CELLS

Measurements were made using an automatic network analyzer to determine the network scattering (S), parameters for a number of TEM cells as a function of frequency. These S-parameters comprise a total characterization of the cell as a two terminal network from which the cell's complex impedance, insertion loss, and resonant frequencies can be determined.

13

The operational details of the system used to make these measurements has been published [17] and are not repeated here. However, the test system's functional diagram is shown in figure 3. The system has three main sections, namely, source, measurement, and computer. The signal generator provides the RF power over the frequency range of interest (0.1 GHz and above) required to pre-calibrate the system and test the unknown device or the TEM cells. The frequency and level of the RF source is stabilized, level controlled, and pre-selected by command to the computer. The RF is applied to the device under test via the S-parameter test set. Then depending upon how S_1 and S_2 are set, the parameters S_{11}, S_{22}, S_{12}, or S_{21} are measured.

The "complex ratio detector" measures the amplitude ratio and phase difference between the reference and test channels. This information is digitized and routed to the computer via the instrument interface.

The computer then takes the S-parameter data and stores it either as calibration data, if measuring standards, or raw, corrected data if measuring the TEM cell. This data is then processed for correction and routed to the displays and to other computer peripherals.

Summarizing, the measurement sequence essentially is broken into two steps. The first is the preparation of the system through pre-calibration to make the desired measurement. The second is to measure, digitize, and store the S-parameter data in the computer and then convert, correct, and output the data in the desired form. Examples of data obtained for a typical TEM cell are given in figure 4. Resonant frequencies are indicated by the high VSWR. Note how narrow the bandwidth is for each resonance. This is indicative of the small RF losses within the cell's conductive walls and center plate and is an indication of the cell Q factor.

6. RESULTS AND CONCLUSIONS

In this section we will discuss the result obtained for the resonant frequency of the first higher-order, perturbed mode in a TEM cell with a symmetrically placed center septum via three different techniques; 1) the experimental measurement as described in the last section, 2) theoretical calculations based upon (69), and 3) a numerical result based upon an exact integral equation formulation as obtained from equation (58) in the work of Mittra and Itoh [4]. In both of the last two methods, the cutoff frequency, f_c, is actually calculated, and this must then be converted to the resonant frequency, f_{res}, via the following well known result

$$f_{res} = [f_c^2 + (\frac{c}{2d})^2]^{\frac{1}{2}} \tag{86}$$

where

$$c = 1/\sqrt{\mu_o \epsilon_o} \; ; \tag{87}$$

and d is the resonant length.

As shown in the figure included with table 1, the two ends of the TEM cell are tapered, so that the resonant length is not very well defined. As a first approximation, however, we will take the average overall length as the resonant length.

In order to find the zero of (69), a root-finder based upon the bisection method was used. This is contained in the Appendix. This same root-finder was also used to find the zeroes of Mittra and Itoh's equation (58), which for a symmetrically-placed center septum and a homogeneous dielectric filling reduces to the following for the TE modes

$$\left(1 - \frac{Y_1(0)}{\hat{k}_1} K_1\right) = 0 \tag{88}$$

where

$$K_1 = \alpha_2 = \frac{1}{2}(1 + \cos\frac{\pi w}{a}); \tag{89}$$

and

$$\frac{Y_1(0)}{\hat{k}_1} = \frac{S_1'(0) + 2d_1(0)E_1}{\hat{k}_1[S(0) - 2I_g]}. \tag{90}$$

The symbols in the above equations are defined in Mittra and Itoh's paper and in general must be evaluated numerically. However, for a small gap, it can be shown that the solution of (88) is given approximately by

$$S(0) - 2I_g = 0 \tag{91}$$

or just the denominator of (90) equal to zero. Note that $K_1 \to 0$ in (88) as $w \to a$. Furthermore (91) can be shown to reduce to our result given in (69) for $g/a \to 0$.

Shown in figure 5 are the calculated cutoff wavelengths computed via Mittra and Itoh's eq. (58) and our result, eq. (69) for two different TEM cell geometries. As expected, the two curves become indistinguishable for very small gaps. The w/a ratios of the TEM cells currently being used at NBS are all greater than 0.72. Thus figure 5 shows that only a few percent error occurs even for those cells with the largest gaps. It is also interesting to note that Mittra and Itoh's result predicts a cutoff wavelength given by that of the TE_{11} mode in the full cell for septum widths up to nearly half of the width of the cell.

Shown in table 1 are the calculated and experimentally measured resonant frequencies of the first higher-order, perturbed mode in nine different TEM cells used at NBS. The column labeled "Form Factor Group" refers to those cells which are scaled versions of one another. As can be seen, the largest percentage error between our approximate solution and the measured value is 6.4% for w/a = .72 or g/a = 0.28. For smaller gaps (w/a = .83) the percentage difference is typically 1%.

Thus we are able to predict the useful frequency range of a TEM cell within a few percent. Using the same technique, additional work needs to be done to extend our solution to TEM cells which have different dielectrics above and below the center septum, i.e., a shielded strip line. In addition, if we reformulate the problem in terms of an integral equation for the current on the septum, then we should be able to obtain an equivalent form for small center septums, i.e., w/a << 1. The formulation of the problem for TM modes has yet to be accomplished. When this is completed, we should be able to look at the TEM mode solution (a degenerate TM mode) and obtain a formula for the characteristic impedance of a TEM cell with an off-center septum. Thus, the solution of the conventional strip-line problem can be obtained by the same technique described in this report.

7. REFERENCES

[1] Tippet, J.C. and D.C. Chang, "Radiation characteristics of dipole sources located inside a rectangular , coaxial transmission line," NBSIR 75-829 (Jan. 1976).

[2] Mittra, R, "Relative convergence of the solution of a doubly infinite set of equations," J. Res. Nat. Bur. Stand. (U.S.), 67D, (Radio Propagation) No. 2, 245-254 (March-April 1963).

[3] Jones, D.S., The Theory of Electromagnetism, pp. 566-569 (Pergamon Press, New York, N.Y., 1964).

[4] Mittra, R. and T. Itoh, "A new technique for the analysis of the dispersion characteristics of microstrip lines," IEEE Trans. on MTT, Vol. MTT-19, No. 1, 47-56 (Jan. 1971).

[5] Bräckelmann, W., D. Landmann, and W. Schlosser, "Die grenzfrequenzen von höheren eigenwellen in streifenleitungen," Arch. Elek. Ubertragungstech., Vol. 21, No. 3, 112-120 (March 1967).

[6] Bezlyudova, M.M., "Cutoff wavelength of waveguide-type oscillations in transmission lines having internal and external conductors of rectangular cross section," Radio Engineering and Electronic Physics, Vol. 8, No. 11 1727-1733 (Nov. 1963).

[7] Kopp, E.H., "Coupling between dissimilar waveguides," IEEE Trans. on MTT, Vol. MTT-16, No. 1, 6-11 (Jan. 1968).

[8] Friedman, B., Principles and Techniques of Applied Mathematics, p. 271 (Wiley, New York, N.Y., 1956).

[9] Jackson, J.D., Classical Electrodynamics, p. 15 (Wiley, New York, N.Y., 1962).

[10] Lewin, L., Theory of Waveguides (Newnes-Butterworths, London, 1975).

[11] Mitta, R., T. Itoh, and T.-S. Li, "Analytical and numerical studies of the relative convergence phenomenon arising in the solution of an integral equation by the moment method," IEEE Trans. on MTT, Vol. MTT-20, No. 2, 96-104 (Feb. 1972).

[12] Collin, R.E., Field Theory of Guided Waves, p. 581 (McGraw-Hill, New York, N.Y., 1960).

[13] Jolley, L.B.W., Summation of Series, pp. 96, 97 (Dover Publ. Inc., New York, N.Y., 1961).

[14] Chang, D.C., "Equivalent-circuit representation and characteristics of a radiating cylinder driven through a circumferential slot," IEEE Trans. on Antennas and Propagation, Vol. AP-21, No. 6, 792-796 (Nov. 1973).

[15] Voytovich, N.N., B.Z. Katsenelenbaum, and A.N. Sivov, "The excitation of a two-dimensional metal cavity with a small opening (slotted cylinder)," Radio Engineering and Electronic Physics, Vol. 19, No. 12, 8-17 (Dec. 1974).

[16] Gradshteyn, I.S. and I.M. Ryzhik, Table of Integrals Series and Products, p. 419 (Academic Press, New York, N.Y., 1965).

[17] Rytting, D.K. and S.N. Sanders, "A system for automatic network analysis," Hewlett-Packard Journal, Vol. 21, No. 6, 2-10 (Feb. 1970).

```
      SUBROUTINE ROOT(A,B,F,X,JMAX,E,EI)

C     THIS SUBROUTINE USES THE BISECTION METHOD TO SOLVE FOR ONE ODD
C     ROOT OF F(X) = 0 ON THE INTERVAL (A,B).  THE FUNCTION PASSED
C     THROUGH F MUST BE DECLARED EXTERNAL IN ALL CALLING PROGRAMS.  E IS
C     INTERVAL OF UNCERTAINTY DESIRED FOR THE ROOT, AND MUST BE SMALLER
C     THAN THE STARTING INTERVAL, W = B-A.  THE NUMBER OF BISECTIONS IS
C     DETERMINED BY NMAX = LN(W/E)/LN(2).  AFTER BISECTING, THE FUNCTION
C     VALUE IS COMPARED TO EI.  IF ABS(F(X0)) > EI THEN THE SUBROUTINE
C     PRINTS: DISCONTINUITY AT X = X0.  A RANDOM SEARCH OCCURING JMAX
C     TIMES IS USED TO LOOK FOR A CHANGE OF SIGN IF SIGN(F(A)) =
C     SIGN(F(B)).

      REAL LN2
      DIMENSION Y(3)

C     QUESTION: DOES F(A) = 0.

      YI=F(A)
      IF(YI.NE.0.) GOTO 10
      X=A
      GOTO 80

C     QUESTION: DOES F(B) = 0.

   10 Y2=F(B)
      IF(Y2.NE.0.) GOTO 20
      X=B
      GOTO 80

C     QUESTION: ARE THE SIGNS OF F(A) AND F(B) DIFFERENT.

   20 I1=SIGN(1.,YI)
      I2=SIGN(1.,Y2)
      W=B-A
      IF(II.NE.I2) GOTO 60

C     SEARCH FOR A CHANGE IN SIGN.

      DO 30 J=1,JMAX
      X=A+RANF(0.)*W
      I3=SIGN(1.,F(X))
      IF(I3.NE.I1) GOTO 50
   30 CONTINUE
      PRINT 40
   40 FORMAT(1X*NO CHANGE OF SIGN FOUND*/)
      RETURN
   50 B=X

C     DETERMINE NUMBER OF BISECTIONS

   60 LN2=0.693147181
      NMAX=ALOG(W/E)/LN2+1.
      Y(2+I1)=A
      Y(2-I1)=B

C     BEGIN BISECTION

      DO 70 N=1,NMAX
      X=(Y(1)+Y(3))/2.
      Y3=F(X)
      IF(Y3.EQ.0.) GOTO 80
      I3=SIGN(1.,Y3)
   70 Y(2+I3)=X
   80 IF(ABS(F(X)).LE.EI) GOTO 85

C     CONVERGENCE TO A DISCONTINUITY

      PRINT 82,X
   82 FORMAT(1X*DISCONTINUITY AT X = *EI2.4/)
      RETURN

C     CONVERGENCE TO A ROOT

   85 PRINT 90,X
   90 FORMAT(1X*ONE ODD ROOT AT X = *EI2.4/)
      RETURN

      END
```
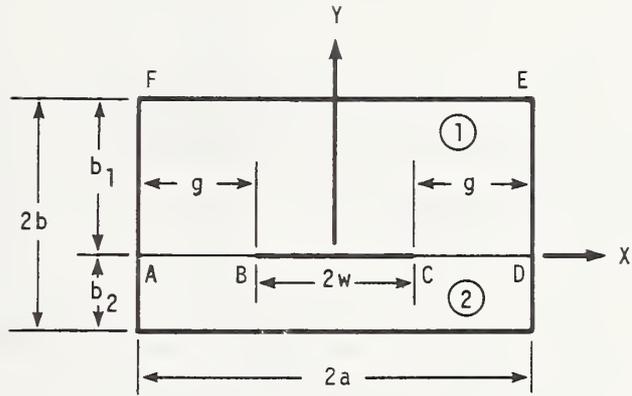
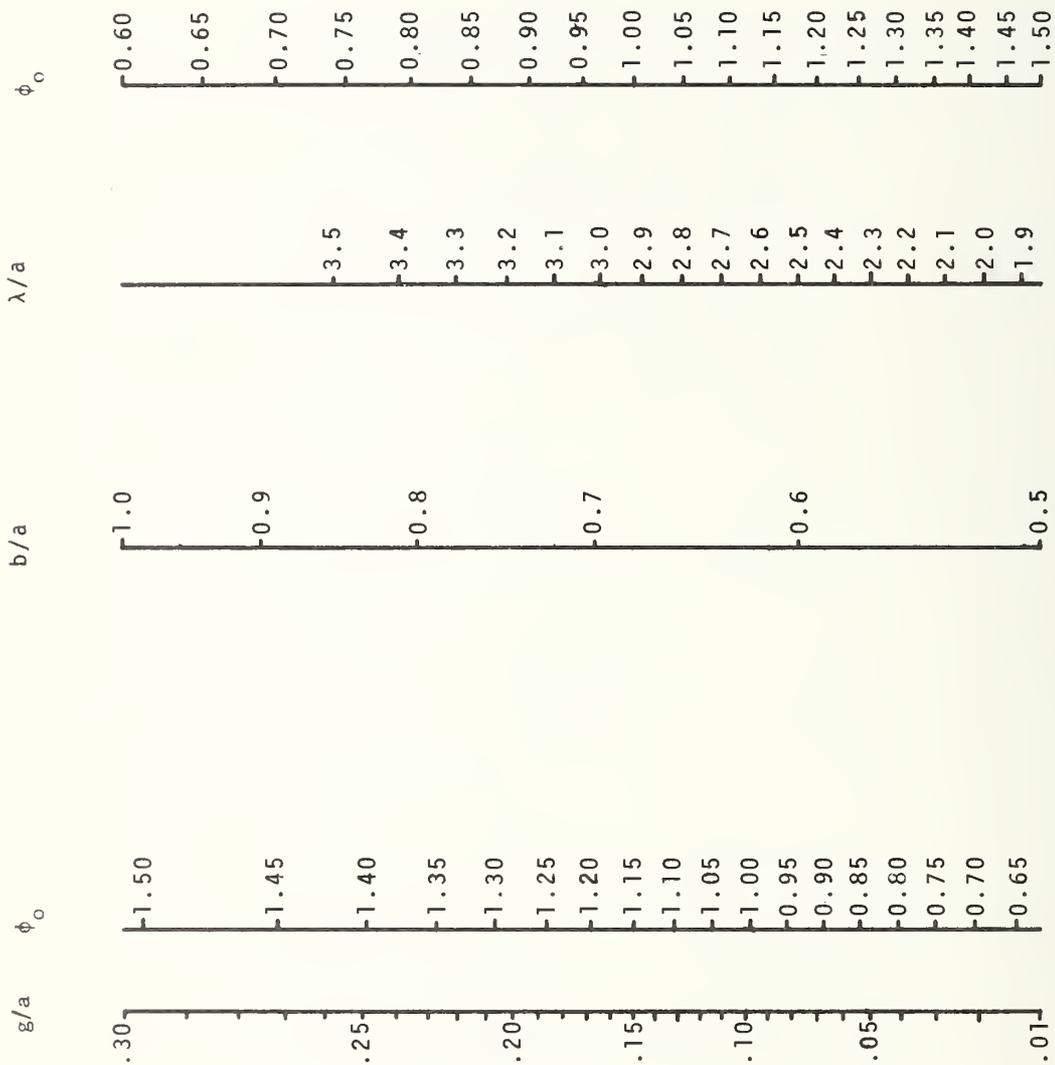Figure 1. Cross-section of a TEM cell.

g/a   φ₀   b/a   λ/a   φ₀

g/a ϕ_o

.30 —

.25 —

.20 —

.15 —

.10 —

.05 —

.01 —

ϕ_o

1.50
1.45
1.40
1.35
1.30
1.25
1.20
1.15
1.10
1.05
1.00
0.95
0.90
0.85
0.80
0.75
0.70
0.65

b/a

1.0
0.9
0.8
0.7
0.6
0.5

λ/a

3.5
3.4
3.3
3.2
3.1
3.0
2.9
2.8
2.7
2.6
2.5
2.4
2.3
2.2
2.1
2.0
1.9

ϕ_o

0.60
0.65
0.70
0.75
0.80
0.85
0.90
0.95
1.00
1.05
1.10
1.15
1.20
1.25
1.30
1.35
1.40
1.45
1.50

Figure 2. Nomograph for determining the cutoff wavelength of the first higher-order perturbed
mode in a TEM cell given the ratios g/a and b/a.

20

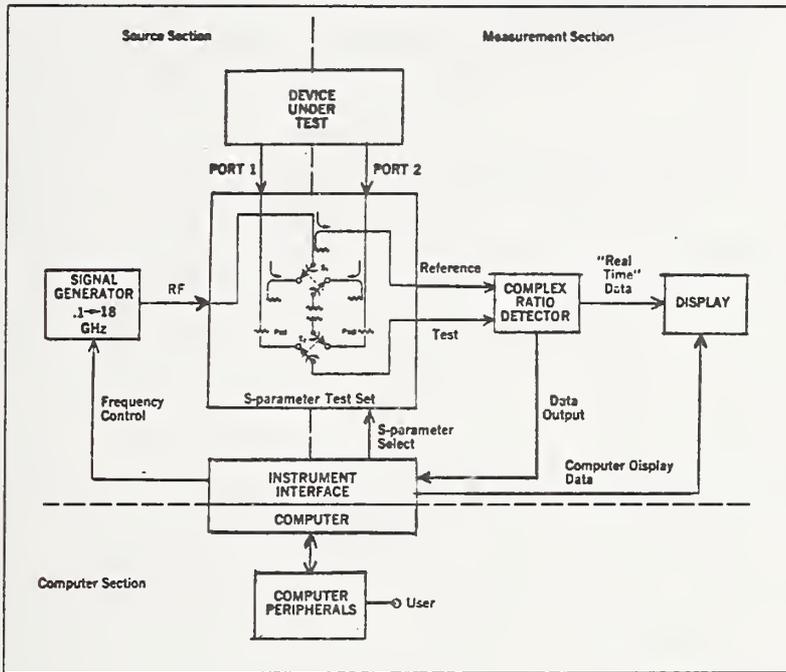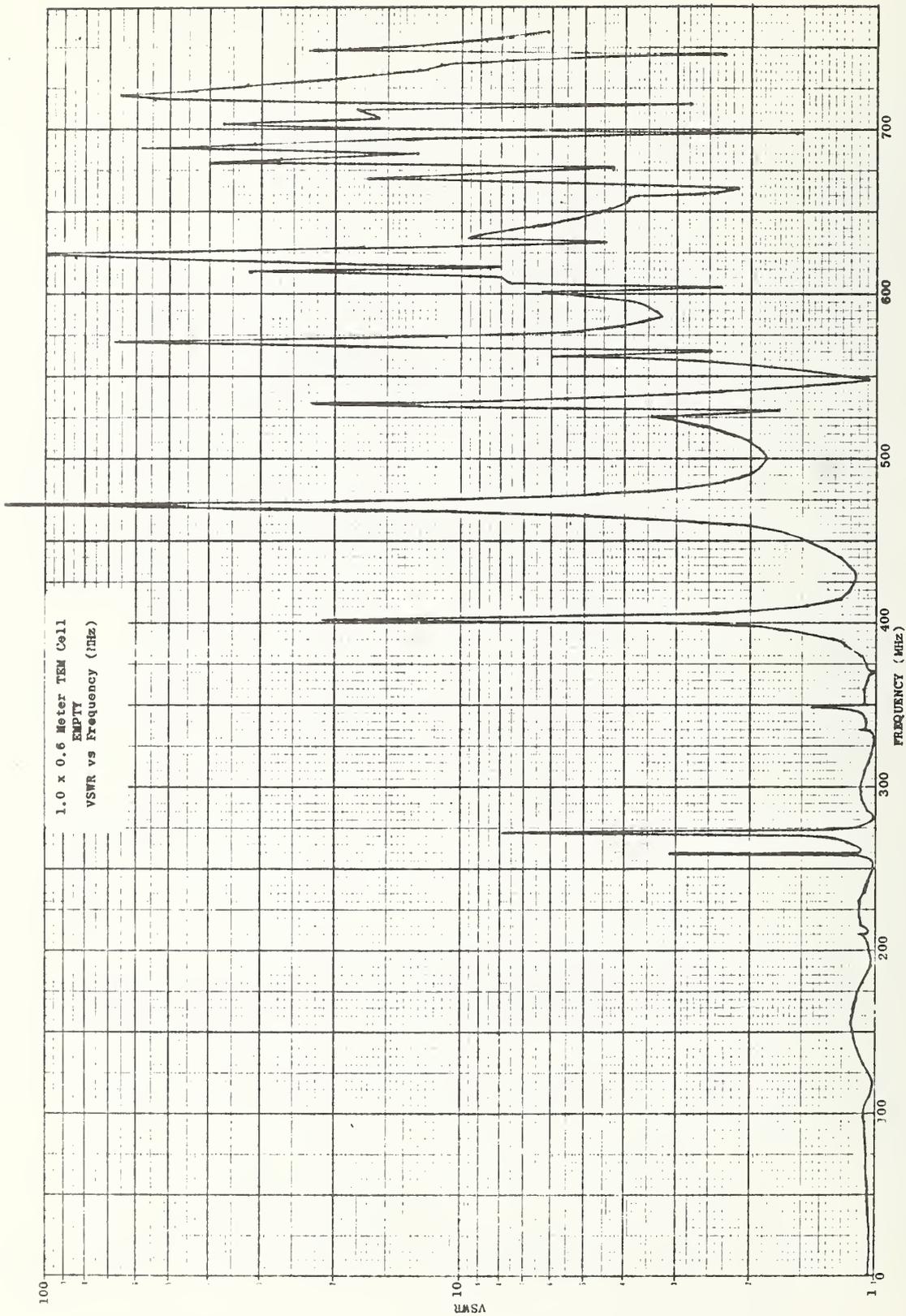Figure 3. Functional diagram of an automatic network analyzer (ANA) system.

Figure 4. Typical data obtained from an automatic network analyzer.

22

UNPERTURBED TE$_{10}$ MODE

MITTRA & ITOH'S SOLUTION

APPROXIMATE SOLUTION FOR SMALL GAP (g/a <<1)

TE$_{11}$ MODE OF THE FULL GUIDE

CUTOFF WAVELENGTH VS SEPTUM WIDTH OF THE FIRST HIGHER ORDER PERTURBED MODE IN A TEM CELL

λ/a

$2\sqrt{2}$

a = b = 1

g ◄ 2w ► g, 2b, 2a

$\dfrac{w}{a}$
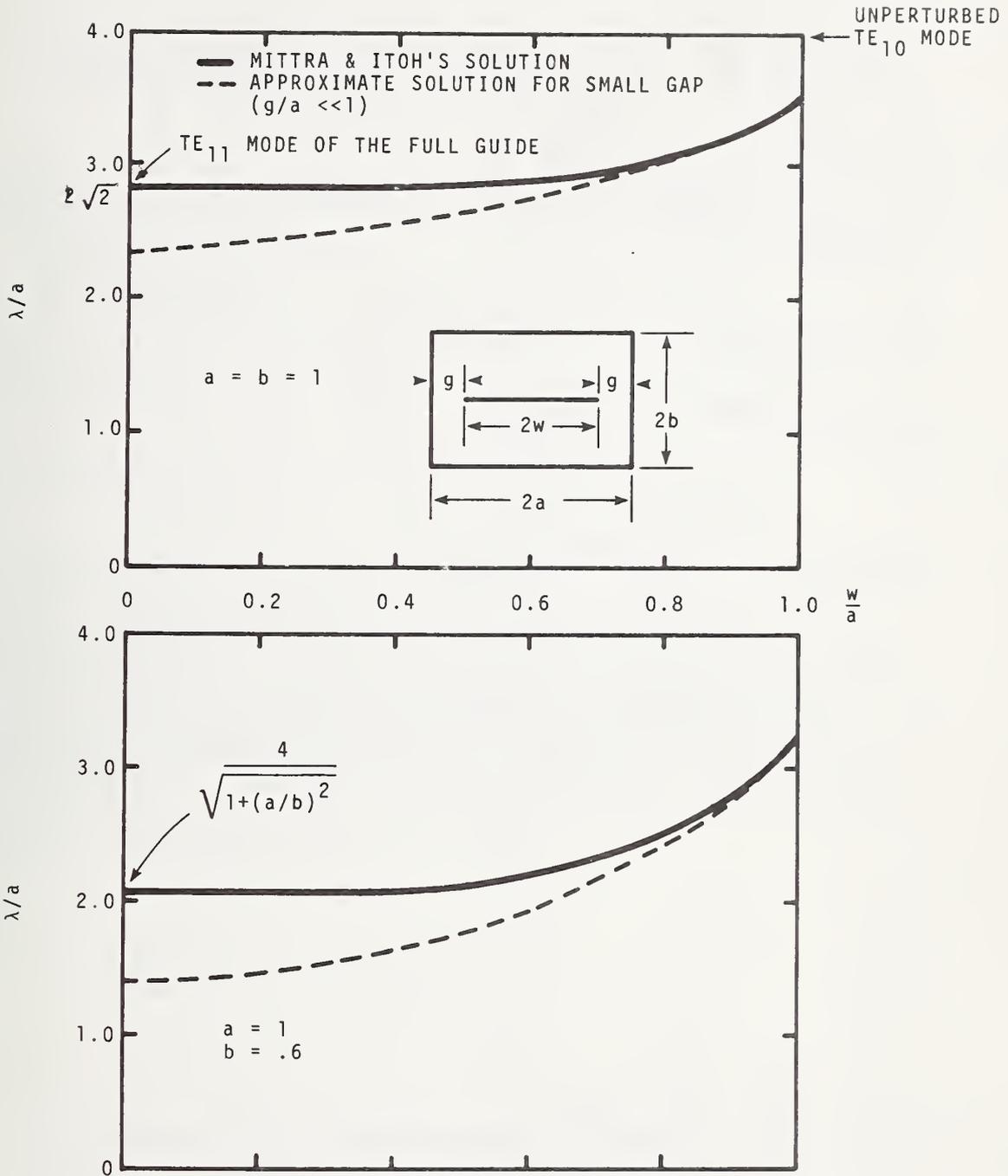
$\sqrt{\dfrac{4}{1+(a/b)^2}}$

λ/a

a = 1
b = .6

re 5. Comparison of Mittra and Itoh's exact solution and our approximate solution for the cutoff wavelength of the first higher-order perturbed mode in a TEM cell.
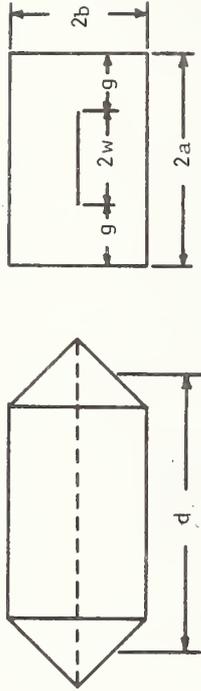
23

Table 1. Calculated and measured resonant frequencies of the first higher-order perturbed mode in nine different NBS TEM cells.

$$f_c \cong f_o \sqrt{1 + (2R_1\phi_o)^2}$$

where $\cot\phi_o = R_1[\ln R_2 - 2]\phi_o$; $f_o = \dfrac{c}{4a}$;

$R_1 = \dfrac{a}{b\pi}$; $R_2 = \dfrac{8a}{\pi g}$; and $\phi_o = b\delta_{10}$

$$f_{res} = \sqrt{f_c^2 + \left(\dfrac{c}{2d}\right)^2}$$

Cell number	2a (cm)	$\frac{a}{b}$	$\frac{w}{a}$	$\frac{d}{a}$	Form Factor Group	fc (MHz) Approx	Δfc %	fc (MHz) Mittra	fres (MHz) Approx	Δfres %	fres (MHz) Exp	Δfres %	fres (MHz) Mittra
1	600.	1.0	.83	3.0	I	32.4	1.25	32.0	36.4	–	–	–	36.1
2	25.4	1.0	.83	3.0	I	765.3	1.3	755.4	860.6	1.2	850.	.2	851.8
3	42.34	1.7	.72	3.0	II	639.0	6.5	599.8	681.3	6.1	640.	.7	644.6
4	50.	1.7	.72	3.0	II	541.4	6.6	508.1	577.2	6.4	540.	1.1	546.0
5	100.	1.7	.72	3.0	II	270.4	6.5	253.9	288.3	6.3	270.	1.1	272.9
6	30.	1.5	.76	3.0	III	813.1	4.3	779.6	878.8	–	–	–	847.9
7	90.	1.5	.76	3.0	III	270.1	4.2	259.2	292.1	2.4	285.	1.1	282.0
8	50.8	1.0	.83	4.75	IV	382.6	1.3	377.7	402.3	.6	400.	.6	397.6
9	121.92	1.0	.82	4.0	V	160.0	1.3	157.9	171.4	<1.4	169.-172	<1.5	169.5

NPS-114A (REV. 7-73)

4. TITLE AND SUBTITLE		5. Publication Date
An Analytical and Experimental Determination of the Cutoff Frequencies of Higher-Order TE Modes in a TEM Cell		July 1976
		6. Performing Organization Code 276.06

7. AUTHOR(S) John C. Tippet, David C. Chang, and Myron L. Crawford	8. Performing Organ. Report No.

9. PERFORMING ORGANIZATION NAME AND ADDRESS	10. Project/Task/Work Unit No. 2766281
NATIONAL BUREAU OF STANDARDS DEPARTMENT OF COMMERCE WASHINGTON, D.C. 20234	11. Contract/Grant No.

15. SUPPLEMENTARY NOTES

16. ABSTRACT (A 200-word or less factual summary of most significant information. If document includes a significant bibliography or literature survey, mention it here.)

In addition to the TEM mode, higher order TE and TM modes can propagate in a TEM cell. Since only the TEM mode is desired, the higher-order modes restrict the useful frequency range of the TEM cell. In this paper, the cutoff frequency of the first higher-order mode is obtained both analytically and experimentally for several TEM cells of differing geometry. The difference between the experimental and theoretical results is shown to be only a few percent. In addition the field distribution of the first higher-order mode is found explicitly.

17. KEY WORDS (six to twelve entries; alphabetical order; capitalize only the first letter of the first key word unless a proper name; separated by semicolons)

Shielded strip line; TEM cell.

18. AVAILABILITY ☒ Unlimited	19. SECURITY CLASS (THIS REPORT)	21. NO. OF PAGES
☐ For Official Distribution. Do Not Release to NTIS	UNCLASSIFIED	28
☐ Order From Sup. of Doc., U.S. Government Printing Office Washington, D.C. 20402, SD Cat. No. C13	20. SECURITY CLASS (THIS PAGE)	22. Price
☒ Order From National Technical Information Service (NTIS) Springfield, Virginia 22151	UNCLASSIFIED	$4.00

USCOMM-DC 29042-P74
USCOMM - ERL